Oral Oncology 93 (2019) 101–106

Contents lists available at ScienceDirect

Oral Oncology

journal homepage: www.elsevier.com/locate/oraloncology

Chemoradiotherapy-related carotid artery inflammation in head and neck cancer patients quantified by [^{18}F]FDG PET/CT☆

Xuguang Chen[a], Yiran Zheng[b], Curtis Tatsuoka[b], Raymond F. Muzic Jr[d], Christian C. Okoye[e], James K. O'Donnell[f], David Zidar[g], Norbert Avril[f], Guilherme H. Oliveira[h], Hongyan Liu[c], Jessica Bucher[b], Mitchell Machtay[b], Min Yao[b], Jennifer A. Dorth[b,*]

[a] Department of Radiation Oncology, Johns Hopkins University School of Medicine, Baltimore, MD, United States
[b] Department of Radiation Oncology, University Hospitals Seidman Cancer Center, Case Western Reserve University, Cleveland, OH, United States
[c] Department of Neurology, University Hospitals Cleveland Medical Center and Department of Population and Quantitative Health Sciences, Case Western Reserve University, Cleveland, OH, United States
[d] Department of Radiology, University Hospitals Cleveland Medical Center, Case Center for Imaging Research, Case Western Reserve University, Cleveland, OH, United States
[e] Department of Radiation Oncology, St. Bernards Medical Group, Jonesboro, AR, United States
[f] Department of Radiology, University Hospitals Cleveland Medical Center, Case Western Reserve University Cleveland, OH, United States
[g] Harrington Heart and Vascular Institute, Department of Medicine, University Hospitals, Case Western Reserve University, Cleveland, OH, United States
[h] Onco-Cardiology Program, and Advanced Heart Failure and Transplant Center, Harrington Heart and Vascular Institute, Department of Medicine, University Hospitals, Case Western Reserve University, Cleveland, OH, United States

ARTICLE INFO

Keywords:
Inflammation
Head and neck cancer
Radiation therapy
PET/CT imaging
Fluorodeoxyglucose (FDG)

ABSTRACT

Objectives: Radiotherapy (RT) is associated with an increased risk of cardiovascular disease (CVD), but little is known about the mechanism for vascular injury and methods for early detection.

Materials and methods: We conducted a prospective, pilot study of carotid artery inflammation using ^{18}F-labeled 2-fluoro-2-deoxy-D-glucose ([^{18}F]FDG) PET/CT imaging pre- and 3 months post-RT in head-and-neck cancer (HNC) patients. [^{18}F]FDG uptake by the carotid arteries was measured by the maximum and mean target to background ratio (TBR_{MAX}, TBR_{MEAN}) and the mean partial volume corrected standardized uptake value ($pvcSUV_{MEAN}$).

Results: Of the 22 patients who completed both pre and post-RT scans, the majority (82%) had stage III or stage IV disease and received concurrent chemotherapy. TBR_{MAX}, TBR_{MEAN}, and $pvcSUV_{MEAN}$ were all significantly higher 3 months after RT versus before RT with mean difference values (95% CI; *p*-value) of 0.17 (0.1–0.25; 0.0001), 0.19 (0.12–0.25; 0.0001), and 0.31 g/ml (0.12–0.5; 0.002), respectively. Fifteen patients (68%) had HPV-positive tumors, which were associated with lower pre-RT [^{18}F]FDG signal, but a greater increase in TBR_{MAX} (19% vs 5%), TBR_{MEAN} (21% vs 11%) and $pvcSUV_{MEAN}$ (20% increase vs 3% decrease), compared to HPV negativity.

Conclusion: There is a significant increase in carotid artery inflammation in HNC patients due to CRT that amounts to a degree that has previously been associated with higher risk for future CVD events. The subset of patients with HPV-positive tumors experienced the greatest increases in vascular inflammation due to CRT. Carotid [^{18}F]FDG uptake may be an early biomarker of RT-related vascular injury.

Abbreviations: FDG, fluorodeoxyglucose; HNC, head and neck cancer; CVD, cardiovascular disease; PVC, partial volume correction; RT, radiotherapy; US, ultrasound; HPV, human papillomavirus; Gy, Gray; CECT, contrast-enhanced CT; ROI, region of interest

☆ Research reported in this publication was supported by the National Cancer Institute of the National Institutes of Health under Award Number K12CA076917. The content is solely the responsibility of the authors and does not necessarily represent the official views of the National Institutes of Health.

* Corresponding author at: Department of Radiation Oncology, Case Western Reserve University School of Medicine, 11100 Euclid Avenue, Lerner Tower B-181, Cleveland, OH 44106.
E-mail address: jennifer.dorth@uhhospitals.org (J.A. Dorth).

https://doi.org/10.1016/j.oraloncology.2019.04.008
Received 28 December 2018; Received in revised form 2 April 2019; Accepted 5 April 2019
Available online 01 May 2019
1368-8375/

Introduction

While radiotherapy (RT) improves survival for many cancer patients, it also leads to an increased risk of cardiovascular disease (CVD) including stroke and heart attack in survivors of head and neck cancer (HNC), lung cancer, breast cancer, and Hodgkin lymphoma [1–4]. HNC patients have a 5-year stroke rate of 12–32% after undergoing cancer treatment, related to the effects of RT and underlying cardiovascular risk that can lead to carotid artery stenosis [5,6]. Post-irradiation carotid stenosis is more aggressive and refractory to therapy [7–9] with higher rates of progression (66% vs. 5% per year) [10,11] and development of restenosis after stenting (88% vs. 27% over two years), compared to non-irradiated patients with stenosis [10,12]. Given the difficulty in treating RT-related carotid artery stenosis and preventing future stroke, it is critical to better understand the pathophysiology of this process and develop early detection and prevention strategies.

[^{18}F]FDG PET/CT is an important tool for imaging vascular inflammation. Vascular metabolic activity detected by [^{18}F]FDG PET/CT is specifically confined to areas of macrophage/monocyte infiltration in the vessel wall based histopathology studies of patients with carotid stenosis who undergo carotid endarterectomy [13,14]. In further support, a higher degree of [^{18}F]FDG uptake in the ascending aorta of patients with HIV infection (compared to controls matched for Framingham risk) correlates with increased soluble CD163, a marker of activated monocytes and macrophages [15]. In the *ApoE*$^{-/-}$ mouse model of atherosclerosis, aortic [^{18}F]FDG uptake correlated with detection of macrophage lineage markers as well as monocyte/macrophage cell adhesion molecules (CAMs) [16].

Moreover, vascular inflammation detected by PET/CT is associated with an increased risk of cardiovascular events [17]. A recent meta-analysis of 14 studies involving 539 patients confirmed a significant association between higher [^{18}F]FDG uptake and symptomatic versus asymptomatic carotid atherosclerotic disease [18]. In a prospective study of 334 patients undergoing [^{18}F]FDG PET/CT for cancer staging, the baseline carotid metabolic activity was significantly higher among patients who developed a stroke versus those who did not during a median of 2.5 years of follow-up time (maximum target-to-background ratio (TBR_{max}): 1.6 vs. 1.18) [19].

There is evidence that RT-related vascular injury has an inflammatory component at both early and late time points. Preclinical studies demonstrate endothelial upregulation of cell adhesion molecules that bind inflammatory cells within 24 hours of RT [20,21]. There is also evidence that vascular inflammatory processes may continue to occur up to 10 years after RT based on biopsies of human cervical arteries [22]. We therefore hypothesized that [^{18}F]FDG PET/CT may detect sub-acute inflammation in irradiated carotid arteries of HNC patients as early as three months following treatment. PET/CT scans are performed as standard of care at three months after completion of RT to assess for residual cancer once the majority of acute, RT-related tumor inflammation has resolved [23].

Methods and materials

This prospective pilot study, CASE 8313, was approved by the University Hospitals Cleveland Medical Center Institutional Review Board and enrolled patients with HNC (squamous cell or adenocarcinoma) from 2014 to 2016. All patients gave written informed consent and underwent pre- and three-month post-RT [^{18}F]FDG PET/CT scans on a standardized imaging protocol. Inclusion criteria were defined as patients undergoing definitive or adjuvant (chemo)radiation with curative intent. All participants were treated with prescribed doses ranging from 50 to 70 Gray (Gy) to target one or more neck lymph node regions using intensity-modulated radiation therapy (IMRT). Exclusion criteria included a history of prior radiation to the head or neck, autoimmune or vasculitic disease, human immunodeficiency virus (HIV) infection, or ongoing use of an immunosuppressive therapy including steroids. Patients were also excluded if they had a history of a cerebrovascular event. We estimated the 10-year risk for developing a cardiovascular disease (CVD) event for each patient according to a simplified Framingham model that does not require laboratory testing [24].

Imaging protocol

[^{18}F]FDG PET/CT and contrast-enhanced CT (CECT) scans were obtained using a standardized protocol at diagnosis and three months after the completion of RT. All scans were acquired with patients wearing a thermoplastic head holder in the radiation treatment position. Patients fasted at least four hours prior to the injection of [^{18}F]FDG, and their serum glucose was verified to be within the normal range less than 120 mg/dl before injection. A total of 10–20 mCi (or 370–740 GBq) of [^{18}F]FDG was injected for every patient. PET/CT scans were performed sixty minutes (± 10 minutes) after [^{18}F]FDG injection on a Phillips Gemini TF large bore PET/CT, a version of the Gemini TF that has an expanded patient aperture but that otherwise has equivalent performance [25]. Dedicated head and neck imaging was acquired first from the orbits to the bottom of the heart with the patients' arms by their sides and reconstructed using 2 mm voxels. Subsequently, the standard whole body acquisition was performed in the arms-up position and reconstructed using 4 mm voxels. A low-dose CT scan with 1 mm slice thickness for the head-and-neck images and 5 mm for the whole-body images was acquired for attenuation correction. Additionally, CECT scans of the head and neck were acquired with 2–3 mm slice thickness at the time of the CT simulation scan in radiation oncology or concurrently with the three-month post-RT PET/CT on the Phillips Gemini. Recent reports suggest that delayed PET imaging (90–120 min vs. standard 60 min) following [^{18}F]FDG injection may provide higher sensitivity for detection of vascular inflammation [26,27]. Based on these data, a subgroup of our study participants also underwent delayed imaging at 120 ± 10 minutes after injection, in addition to standard timing of sixty minutes.

Image analysis

The low-dose CT scan from the PET/CT and the CECT scans were manually co-registered by aligning anatomic structures near the carotid artery. We manually defined carotid artery ROIs including the entire carotid artery (common carotid extending to the internal carotid), carotid bulb, and expanded bulb plus 2 cm cranial and caudal (Fig. 1). To account for the difference in resolution of the low-dose CT and PET, the PET scans were resampled to the CT matrix with a voxel size of 1 mm. A MIM Maestro platform version 6.7.11 was used to co-register CT scans, manually define ROIs, and for image analysis (MIM Software, Inc., Beachwood, OH).

Mean and maximum standardized uptake values (SUVs, in g/ml) were defined according to standard convention as the decay-corrected tissue concentration of [^{18}F]FDG (in kBq/ml) divided by the injected dose per body weight (in kBq/g) [28]. To minimize the effect of signal contamination from nearby regions containing tumor, the FDG-avid primary tumor or regional lymph nodes plus 1 cm (Fig. 1) were excluded from the carotid ROIs.

We examined multiple [^{18}F]FDG PET-based indices of vascular inflammation using previously published metrics [27,29]. Mean and maximum target-to-background ratios (TBR) (TBR_{MEAN} and TBR_{MAX}) were calculated by dividing the mean and maximum SUVs by the blood pool SUV [29]. Corrected mean and maximum SUVs ($cSUV_{MEAN}$ and $cSUV_{MAX}$) for every slice were calculated by subtracting the blood pool SUV measured in the superior vena cava.

To correct for significant inaccuracies in the activity measurements in the carotid wall caused by it being thin relative to the spatial resolution of PET, the pvcSUV was calculated based on the method described by Bloomberg et al., assuming a carotid wall thickness of 1 mm

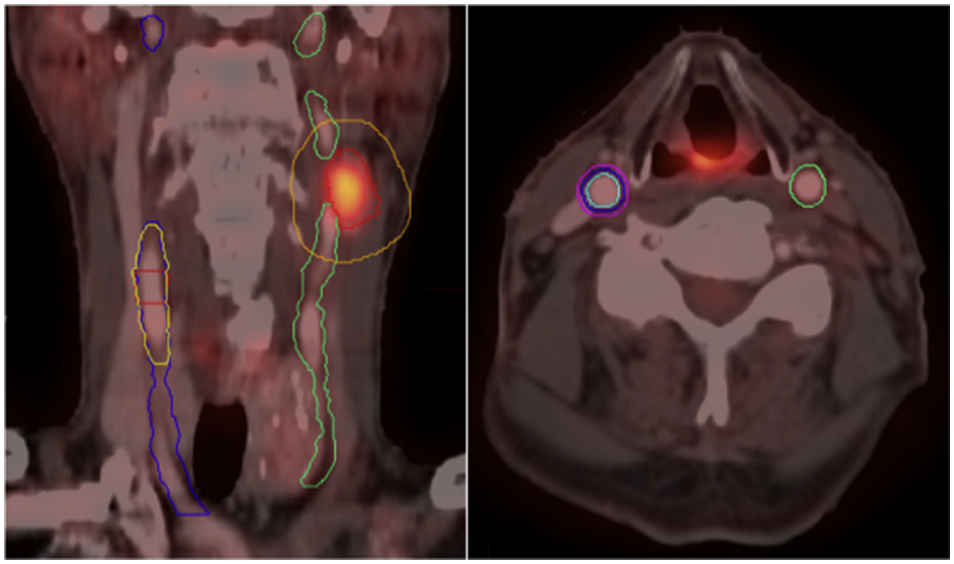

Fig. 1. Carotid artery regions of interest. Carotid artery ROIs delineated on a contrast-enhanced CT fused to a PET/CT. (A) Coronal image depicting the carotid artery from the aortic arch to the base of skull (*blue*: right; *green*: left), carotid bulb (*red*), and expanded carotid bulb plus 2 cm (*yellow*). An FDG-avid lymph node (*red*) was expanded by 1 cm (*orange*) and then subtracted from the final carotid ROIs. (B) Axial image depicting the vessel wall (*blue*: right; *green*: left), spillover area (*magenta*), and arterial lumen (*cyan*). (For interpretation of the references to colour in this figure legend, the reader is referred to the web version of this article.)

[27,30]. In general terms, this method accounts for the spillover activity from the vessel wall while subtracting the blood pool (superior vena cava) and background (erector spinae) activity defined by 1 mm contraction and expansion of the carotid artery contour, respectively.

All of the five PET metrics were measured in all of the three ROIs in the paired pre and post-PET scans because they have been reported on previously and there is not one accepted metric to quantify carotid inflammation due to RT. The values of the [^{18}F]FDG metrics for consecutive axial slices were summed and divided by the number of slices, resulting in single average values for both the right and left carotid arteries for each subject.

Statistical analysis

This study was designed to have at least 80% power to detect a 7% increase in TBR_{MAX} between pre and post-RT carotid arteries with a sample size of 22 patients and assuming two-sided type 1 error of 0.05, 10% attrition, and standard deviation of 10%. The mean and maximum values for cSUV and TBR, as well as the $pvcSUV_{MEAN}$ of the carotid ROIs were calculated. Mixed model analyses were performed with [^{18}F]FDG metrics or change in [^{18}F]FDG metrics as outcomes using linear mixed models in SAS software version 9.4 (SAS Institute, Cary, NC). Subject-level random effects were included. Variables considered for the models were time period (pre vs post-RT) for non-difference outcomes, to assess for change over time. In respective consideration of HPV status, Framingham risk, or statin use as covariates, mixed model outcomes were difference from pre vs. post RT values. Estimated mean difference values by time period and 95% confidence interval (95% CI) are reported. *P*-values less than 0.05 were considered significant.

Results

Patient characteristics

Twenty-two patients were enrolled in the study and completed pre and post-RT PET/CT scans at 1 hour after injection. Of these patients, six also completed scans at 2 hours post injection. An attempt was made to offer study participation to all eligible patients. The most common reason for ineligibility was patients who had already completed staging PET/CT scans prior to their radiation oncology consultation. The baseline characteristics of the 22 study participants by tumor HPV status are presented in Table 1. The majority of patients had stage III or IV disease (96%) per the AJCC 7th edition cancer staging [31] and primary tumor site involving the oropharynx (73%). Fifteen patients (68%) had tumors that were HPV-positive. Patients had an average of 3 cardiovascular risk factors. Seven patients had known hyperlipidemia, of whom five were taking a statin. Patients with HPV-negative tumors had similar Framingham 10-year CVD risk scores compared to HPV-positive tumors (29.4% vs. 25.2%), but there was greater percentage of HPV-negative patients who were active smokers within 3 months of cancer diagnosis (71% vs. 47%) and having a diagnosis of hypertension (71% vs. 33%), compared to HPV-positive patients (Table 1). There was also a higher CVD risk score among patients taking a statin versus those not (mean score: 33.9% vs. 24.4%).

Eighteen patients underwent definitive CRT, two patients underwent definitive RT, and two patients underwent surgical resection followed by radiation. All patients were treated using intensity-modulated

Table 1
Patient characteristics.

Characteristic, n (%)	HPV positive $n = 15$	HPV negative $n = 7$
Gender		
Male	13 (87)	4 (57)
Female	2 (13)	3 (43)
Median age, years (range)	57 (46–72)	60 (50–78)
Cardiovascular risk factors		
Smoking	7 (47)	5 (71)
Diabetes	1 (7)	0
Average Systolic BP	134 mmHg	132 mmHg
Baseline treatment		
Hypertension medication	6 (40)	5 (71)
Statin use	3 (20)	2 (29)
Median 10-year CVD risk (%, range)	25 (6–54)	29 (4–65)
Clinical stage, AJCC 7th edition		
I-II	1 (7)	0
III	3 (20)	2 (29)
IV	11 (73)	5 (71)
Primary site		
Oropharynx	13 (87)	3 (43)
Nasopharynx	2 (13)	0
Larynx	0	2 (29)
Oral cavity	0	1 (14)
Hypopharynx	0	1 (14)
Treatment modalities		
Definitive RT	2 (13)	0
Definitive CRT	13 (87)	5 (71)
Surgery + post-operative RT	0	2 (29)

Table 2
Comparison of pre-RT and post-RT PET metrics among carotid substructures.

Metric anatomic site	Mean value Pre-RT/Post-RT	Mean difference of post-RT minus pre-RT (95% CI)	*p*-value* for mean difference
$cSUV_{MAX}$ (g/ml)			
Entire carotid	1.75 / 1.72	−0.03 (−0.13 to 0.06)	0.50
Bulb + 2 cm	1.94 / 1.84	−0.10 (−0.23 to 0.02)	0.11
$cSUV_{MEAN}$ (g/ml)			
Entire carotid	1.49 / 1.51	0.02 (−0.04 to 0.09)	0.48
Bulb + 2 cm	1.62 / 1.63	0.01 (−0.08 to 0.10)	0.88
TBR_{MAX}			
Entire carotid	1.26 / 1.43	0.17 (0.10 to 0.25)	< 0.0001
Bulb + 2 cm	1.39 / 1.54	0.14 (0.05 to 0.24)	0.004
TBR_{MEAN}			
Entire carotid	1.07 / 1.26	0.19 (0.12 to 0.25)	< 0.0001
Bulb + 2 cm	1.17 / 1.36	0.19 (0.11 to 0.27)	< 0.0001
$pvcSUV_{MEAN}$ (g/ml)			
Entire carotid	2.66 / 2.97	0.31 (0.12 to 0.50)	0.002
Bulb + 2 cm	3.07 / 3.40	0.33 (0.04 to 0.62)	0.03

* Mean *p* value is from mixed model.

radiation therapy to a prescribed dose of 60–70 Gy to the gross disease or post-operative tumor bed/dissected neck, while the uninvolved elective lymph nodal regions received a prescribed dose of 56–63 Gy.

[^{18}F]FDG uptake in the carotid wall after RT

Compliance with the imaging protocol was excellent, with 91% of PET/CT scans initiated within 1 h ± 10 minutes after FDG injection (median: 61 minutes; range: 50–77 minutes). Additionally, all patients had serum glucose levels < 120 mg/dL prior to FDG injection. [^{18}F]FDG PET metrics measured before and after RT are detailed in Table 2. The changes in $cSUV_{MAX}$ and $cSUV_{MEAN}$ were inconsistent for the carotid ROIs, with some values decreasing and others increasing after RT. In contrast, there were consistent increases in TBR_{MAX}, TBR_{MEAN}, and $pvcSUV_{MEAN}$ after RT for the carotid artery and its substructures. For the entire carotid artery, the mean difference value (95% CI; *p*-value) of post-RT minus pre-RT values for the TBR_{MAX}, TBR_{MEAN}, and $pvcSUV_{MEAN}$ was 0.17 (0.1–0.25; 0.0001), 0.19 (0.12–0.25; 0.0001), and 0.31 g/ml (0.12–0.5; 0.002), respectively. This represents a relative increase in these [^{18}F]FDG metrics of 12–18% above pre-RT values. There were similar and statistically significant increases in [^{18}F]FDG metrics including the TBR_{MAX}, TBR_{MEAN}, and $pvcSUV_{MEAN}$ between the entire carotid and expanded carotid bulb, but not for the carotid bulb (data not shown for the bulb). For example, the mean difference (95% CI; *p*-value) in $pvcSUV_{MEAN}$ is 0.31 g/ml (0.12–0.5; 0.002) for the entire carotid and 0.33 g/ml (0.04–0.6; 0.03) for the expanded carotid bulb.

With regards to [^{18}F]FDG metrics obtained from the delayed, 2-hour post-injection scans which were collected in a subset of 6 subjects, there is a numeric increase in $pvcSUV_{MEAN}$ from 2.7 before to 3.0 after RT for the entire carotid with an absolute difference of SUV 0.3 (95% CI: −0.04 to 0.56). In comparison, the 1-hour $pvcSUV_{MEAN}$ among the same 6 patients increased from 2.6 before to 2.8 with an absolute difference of SUV 0.2 (95% CI: −0.76 to 0.40). While the absolute numeric difference was greater for the 2-hour than the 1-hour $pvcSUV_{MEAN}$, neither reached statistical significance, likely reflecting the small sample size.

HPV status and carotid vascular inflammation

We conducted further analysis to determine if baseline [^{18}F]FDG metrics or their post-RT changes differed between patients with HPV-positive and HPV-negative cancers. As shown in Fig. 2, HPV-negative patients had higher absolute values for baseline [^{18}F]FDG uptake compared to HPV-positive patients for TBR_{MAX}, TBR_{MEAN}, and $pvcSUV_{MEAN}$. Specifically, the pre-RT $pvcSUV_{MEAN}$ was 2.5 in HPV-positive patients, compared to 3.1 in HPV-negative patients for the entire carotid. Mixed model analysis demonstrated that HPV-negative status was associated with significantly higher TBR_{MAX} and TBR_{MEAN} values (Table 3), after accounting for time period (pre vs. post-RT) and subject-level effects due to paired carotid arteries. In contrast, there was no association between chemotherapy, 10-year cardiovascular risk or statin use and [^{18}F]FDG metrics in multivariate models (data not shown). In an exploratory analysis, there was no difference in [^{18}F]FDG uptake between carotid arteries located ipsilateral to gross disease in the neck (prescribed a dose of 66–70 Gy) versus arteries without ipsilateral gross disease (prescribed a dose of 56–63 Gy) (data not shown).

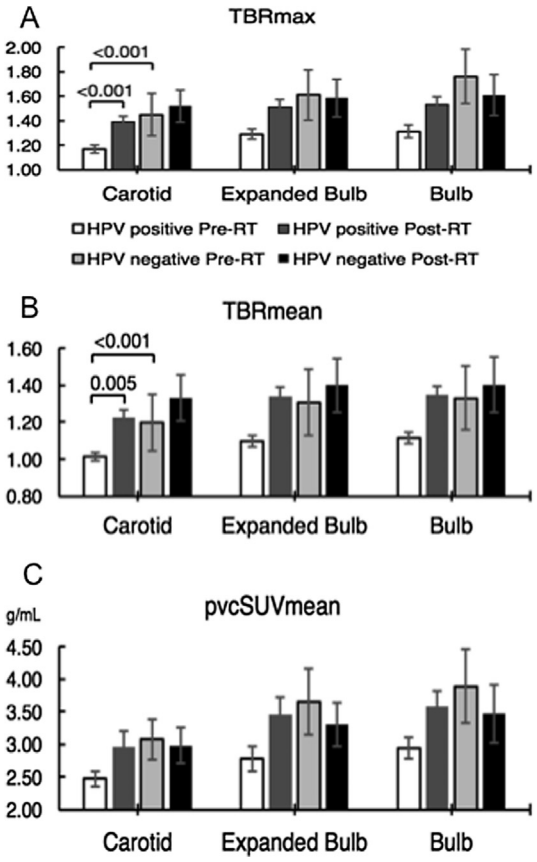

Fig. 2. HPV status and PET metrics. (A) TBR_{MAX}; (B) TBR_{MEAN}; (C) $pvcSUV_{MEAN}$.

While HPV-positive patients had lower carotid FDG uptake at baseline, they experienced greater increases in FDG uptake post RT compared to HPV-negative patients. The estimated mean increase in $pvcSUV_{MEAN}$ for HPV-positive patients was 0.50 (95% CI 0.17–0.82), compared to −0.09 (95% CI −0.57 – 0.39) for HPV-negative patients (Table 4, p = 0.047).

Discussion

Increased carotid artery inflammation due to radiotherapy

Our pilot study is the first prospective study to detect CRT-related changes in vascular inflammation utilizing a standardized [^{18}F]FDG PET/CT imaging protocol and modern quantification of vascular uptake with TBR and pvcSUV metrics that are reproducible and account for partial volume effects [26,27]. We report herein that CRT results in significant increases in carotid inflammation at three months after therapy, the timepoint at which PET/CT scans are obtained to evaluate

Table 3
Multivariate models for PET Metrics with Time Effect and HPV Status.

Metric	Time effect estimate: Post versus pre-RT (95% CI); [*p*-value]	HPV status estimate: Negative versus positive (95% CI); [*p*-value)
TBR_{MAX}	0.17 (0.1–0.25) [< 0.001]	0.21 (0.09–0.32) [0.0007]
TBR_{MEAN}	0.19 (0.12–0.25) [< 0.0001]	0.14 (0.04–0.24) [0.005]
$pvcSUV_{MEAN}$	0.31 (0.12–0.5) [0.002]	0.31 (−0.05–0.67) [0.09]

Table 4
HPV status and RT-associated changes in PET metrics for the entire carotid.

Metric	HPV positive Mean difference of post-RT minus pre-RT (95% CI)	HPV negative Mean difference of post-RT minus pre-RT (95% CI)	*p*-value for HPV status
TBR_{MAX}	0.22 (0.07–0.37)	0.07 (−0.15–0.29)	0.25
TBR_{MEAN}	0.21 (0.07–0.35)	0.13 (−0.07–0.34)	0.51
$pvcSUV_{MEAN}$	0.50 (0.17–0.82)	−0.09 (−0.57–0.39)	0.047

tumor response as part of standard of care. Comparing our results to other studies suggests that the degree of CRT-related increase in vascular inflammation may amount to a clinically-significant injury conferring a higher risk for future CVD events among our HNC patients. Specifically, we found that the TBR_{max} for the expanded carotid bulb increased from 1.39 to a value of 1.54 after CRT (a relative increase of 10.8%). In comparison, a prospective study of unirradiated patients demonstrated higher baseline TBR_{max} of the common carotid artery in patients who experienced a stroke in followup versus those who did not (mean TBR_{max}: 1.6 versus 1.18) [19]. Similar to our results, in a recently published meta-analysis of 14 studies examining carotid FDG uptake between symptomatic and asymptomatic patients found a relative difference of 13.8% [18].

Furthermore, among our patients who underwent delayed PET/CT imaging at 2 hours post [^{18}F]FDG injection, there was an even greater increase in TBR_{max} of the carotid artery from 1.53 to 1.84. This change in carotid metabolic activity due to CRT is comparable to the difference in carotid activity between healthy unirradiated patients versus unirradiated patients with high Framingham CVD risk measured using delayed PET imaging at 90 minutes following [^{18}F]FDG injection (TBR_{max}: 1.55 versus 1.94) [32]. In our study, the change in the 2-hour [^{18}F]FDG metrics were numerically higher than the 1-hour metrics, but statistical analysis was limited by the small sample size of only 6 patients undergoing delayed imaging. Thus, a hypothesis to test using a larger cohort is whether FDG uptake at 2-hour data is more sensitive to change than at one hour.

Another study of irradiated patients suggests that chronic, RT-related vascular inflammation may also be detectable by [^{18}F]FDG PET/CT at 2–3 years after RT [33]. This study found a higher SUV_{max} by a value of 0.42 ($p < 0.05$) in the irradiated carotid or iliac arteries compared to contralateral, non-irradiated vascular segments among 10 lymphoma survivors. Our study expands upon this previous work by assessing an earlier time point after RT, employing a standardized imaging protocol to allow for pre and post-RT comparisons among a uniform group of patients, and utilizing modern quantification of vascular uptake with TBR and pvcSUV metrics.

Predictors of vascular inflammation in HNC patients

We also demonstrated that it may be possible to utilize [^{18}F]FDG PET/CT imaging to identify subgroups of HNC patients at highest risk for developing CRT-related vascular inflammation. Surprisingly, our patients with HPV-negative tumors had higher baseline carotid FDG uptake than HPV-positive tumors (likely related to the greater proportion of patients actively smoking at diagnosis), but patients with HPV-positive tumors experienced greater CRT-related increases in FDG uptake than HPV-negative tumors. It is widely believed that HPV-positive patients have lower traditional cardiovascular risk factors, such as younger age, less use of tobacco and alcohol, and lower rate of comorbidities, such as hypertension and diabetes [34,35]. However, our data suggest that even with similar traditional risk factors, HPV-positive patients may experience significant RT-induced vascular inflammation, which argues for enhanced surveillance of post-RT cerebrovascular disease in this patient population that is sharply growing in number.

Our results may reflect a true difference between these populations, but also may be due to the fact that the majority of the patients in our study (68%) were HPV-positive and therefore there was a greater power to see RT-related changes in this subgroup. Larger studies are needed to confirm this result. However, a recent retrospective analysis supports our finding that HPV tumor positivity may confer a greater risk for vascular injury related to CRT: HPV-positive HNC patients had 4.4 times the risk of cerebrovascular events after RT compared to HPV-negative patients, after adjusting for Framingham risk [36]. Our study offers a potential mechanistic explanation for this elevated cerebrovascular event risk in HPV-positive patients due to greater increases in CRT-related sub-acute inflammation. It is possible that the enhanced systemic and local tumor immune responses seen in patients with HPV-positive tumors could predispose patients to greater vascular inflammation as a consequence of CRT [37].

We did not find a significant association between carotid [^{18}F]FDG uptake and traditional cardiovascular risk and protective factors such as a Framingham score or statin use, respectively, in contrast to other publications demonstrating their association with RT-related vascular injury [10,38]. This may be explained by the following limitations of our study: small sample size of 22 patients with many patients having high baseline risk scores (reflected in a median score of 23%), we had to utilize a simplified Framingham score since we did not have serum LDL cholesterol data, and that many patients had quit smoking more than 3 months before diagnosis but still had a long history of smoking that is not accounted for in the risk calculation.

Study limitations

A limitation of our study is that there was treatment heterogeneity, with some patients undergoing chemotherapy and/or surgery, in addition to radiation. Due to this fact, and the small sample size, it was not possible to assess for an independent effect of surgery or chemotherapy on vascular injury. However, the vast majority (82%) of all patients underwent definitive CRT without surgery and no patients with HPV-positive tumors had surgery (Table 1). This leads us to conclude that the treatment-related increases in vascular inflammation, primarily found among our HPV-positive subset, were due to chemoradiation and not surgery. We were limited in assessing a RT dose-response effect because all patients underwent bilateral neck radiation, the range of prescribed doses to the neck was narrow between 56 and 70 Gy, and only 13 of 22 patients had unilateral neck disease with different doses received by either side of the neck.

Future directions

Our study demonstrates that HNC patients have clinically-significant increases in sub-acute inflammation in the carotid related to CRT. Further studies are needed to correlate imaging biomarkers (such

as [^{18}F]FDG uptake detected by PET/CT and intima-media thickness by carotid ultrasound) and serum inflammatory biomarkers with stroke events in HNC patients. In the short term, carotid [^{18}F]FDG uptake at three months after RT may be an important early biomarker to identify patients at highest risk for stroke and/or to study the impact of therapeutic strategies to prevent injury during RT. Because [^{18}F]FDG PET/CT scans are already obtained at this timepoint as part of standard of care, this imaging assessment of vascular inflammation has the potential to become widely implemented. Furthermore, the fact that we identified a component of sub-acute inflammation due to CRT gives clues as to the pathophysiology of injury and leads us to propose investigating therapies to prevent vascular inflammation, such as statins [39,40].

Conflict of interest statement

None.

Acknowledgements

We are thankful to our colleagues Patrick Wojtylak, Janine Tessean, Leslie Ciancibello, Megan Fontanez, Keith Armstrong, and David Stadnick who provided expertise in implementing specialized imaging protocols for this study in the Departments of Radiology and Nuclear Medicine at University Hospitals Cleveland Medical Center and Lake Health University Hospitals Seidman Cancer Center. This research was also supported by Dr. Fredrick Barton and Michele Snyder-Willis, who enrolled patients and ensured high-quality adherence to the study protocol.

References

[1] Nielsen KM, Offersen BV, Nielsen HM, et al. Short and long term radiation induced cardiovascular disease in patients with cancer. Clin Cardiol 2017;40:255–61.
[2] Wang K, Eblan MJ, Deal AM, et al. Cardiac toxicity after radiotherapy for stage III non-small-cell lung cancer: pooled analysis of dose-escalation trials delivering 70–90 Gy. J Clin Oncol 2017;35:1387–94.
[3] Boivin JF, Hutchison GB, Lubin JH, et al. Coronary artery disease mortality in patients treated for Hodgkin's disease. Cancer 1992;69:1241–7.
[4] Darby SC, Ewertz M, McGale P, et al. Risk of ischemic heart disease in women after radiotherapy for breast cancer. N Engl J Med 2013;368:987–98.
[5] Haynes JC, Machtay M, Weber RS, et al. Relative risk of stroke in head and neck carcinoma patients treated with external cervical irradiation. Laryngoscope 2002;112:1883–7.
[6] Smith GL, Smith BD, Buchholz TA, et al. Cerebrovascular disease risk in older head and neck cancer patients after radiotherapy. J Clin Oncol 2008;26:5119–25.
[7] Orzan F, Brusca A, Conte MR, et al. Severe coronary artery disease after radiation therapy of the chest and mediastinum: clinical presentation and treatment. Br Heart J 1993;69:496–500.
[8] Caro-Codon J, Jimenez-Valero S, Galeote G, et al. Radiation-induced coronary artery disease: Useful insights from OCT. Int J Cardiol 2016;202:535–6.
[9] Cuomo JR, Sharma GK, Conger PD, et al. Novel concepts in radiation-induced cardiovascular disease. World J Cardiol 2016;8:504–19.
[10] Dorth JA, Patel PR, Broadwater G, et al. Incidence and risk factors of significant carotid artery stenosis in asymptomatic survivors of head and neck cancer after radiotherapy. Head Neck 2014;36:215–9.
[11] Abbott AL. Medical (nonsurgical) intervention alone is now best for prevention of stroke associated with asymptomatic severe carotid stenosis: results of a systematic review and analysis. Stroke 2009;40:e573–83.
[12] Protack CD, Bakken AM, Saad WE, et al. Radiation arteritis: a contraindication to carotid stenting? J Vasc Surg 2007;45:110–7.
[13] Tawakol A, Migrino RQ, Bashian GG, et al. In vivo 18F-fluorodeoxyglucose positron emission tomography imaging provides a noninvasive measure of carotid plaque inflammation in patients. J Am Coll Cardiol 2006;48:1818–24.
[14] Rudd JH, Warburton EA, Fryer TD, et al. Imaging atherosclerotic plaque inflammation with [18F]-fluorodeoxyglucose positron emission tomography. Circulation 2002;105:2708–11.
[15] Subramanian S, Tawakol A, Burdo TH, et al. Arterial inflammation in patients with HIV. JAMA 2012;308:379–86.
[16] Hag AM, Pedersen SF, Christoffersen C, et al. (18)F-FDG PET imaging of murine atherosclerosis: association with gene expression of key molecular markers. PLoS ONE 2012;7:e50908.
[17] Paulmier B, Duet M, Khayat R, et al. Arterial wall uptake of fluorodeoxyglucose on PET imaging in stable cancer disease patients indicates higher risk for cardiovascular events. J Nucl Cardiol 2008;15:209–17.
[18] Chowdhury MM, Tarkin JM, Evans NR, et al. (18)F-FDG uptake on PET/CT in symptomatic versus asymptomatic carotid disease: a meta-analysis. Eur J Vasc Endovasc Surg 2018;56:172–9.
[19] Rominger A, Saam T, Wolpers S, et al. 18F-FDG PET/CT identifies patients at risk for future vascular events in an otherwise asymptomatic cohort with neoplastic disease. J Nucl Med 2009;50:1611–20.
[20] Hallahan D, Clark ET, Kuchibhotla J, et al. E-selectin gene induction by ionizing radiation is independent of cytokine induction. Biochem Biophys Res Commun 1995;217:784–95.
[21] Han KH, Ryu JW, Lim KE, et al. Vascular expression of the chemokine CX3CL1 promotes osteoclast recruitment and exacerbates bone resorption in an irradiated murine model. Bone 2014;61:91–101.
[22] Halle M, Gabrielsen A, Paulsson-Berne G, et al. Sustained inflammation due to nuclear factor-kappa B activation in irradiated human arteries. J Am Coll Cardiol 2010;55:1227–36.
[23] Nayak JV, Walvekar RR, Andrade RS, et al. Deferring planned neck dissection following chemoradiation for stage IV head and neck cancer: the utility of PET-CT. Laryngoscope 2007;117:2129–34.
[24] D'Agostino Sr. RB, Vasan RS, Pencina MJ, et al. General cardiovascular risk profile for use in primary care: the Framingham Heart Study. Circulation 2008;117:743–53.
[25] Surti S, Kuhn A, Werner ME, et al. Performance of Philips Gemini TF PET/CT scanner with special consideration for its time-of-flight imaging capabilities. J Nucl Med 2007;48:471–80.
[26] Rudd JH, Myers KS, Bansilal S, et al. Relationships among regional arterial inflammation, calcification, risk factors, and biomarkers: a prospective fluorodeoxyglucose positron-emission tomography/computed tomography imaging study. Circ Cardiovasc Imaging 2009;2:107–15.
[27] Blomberg BA, Akers SR, Saboury B, et al. Delayed time-point 18F-FDG PET CT imaging enhances assessment of atherosclerotic plaque inflammation. Nucl Med Commun 2013;34:860–7.
[28] Shankar LK, Hoffman JM, Bacharach S, et al. Consensus recommendations for the use of 18F-FDG PET as an indicator of therapeutic response in patients in National Cancer Institute Trials. J Nucl Med 2006;47:1059–66.
[29] Rudd JH, Myers KS, Bansilal S, et al. Atherosclerosis inflammation imaging with 18F-FDG PET: carotid, iliac, and femoral uptake reproducibility, quantification methods, and recommendations. J Nucl Med 2008;49:871–8.
[30] Howard G, Sharrett AR, Heiss G, et al. Carotid artery intimal-medial thickness distribution in general populations as evaluated by B-mode ultrasound. ARIC Investigators. Stroke 1993;24:1297–304.
[31] Edge SB. American Joint Committee on Cancer: AJCC cancer staging manual. 7th ed. New York: Springer; 2010.
[32] van der Valk FM, Verweij SL, Zwinderman KA, et al. Thresholds for arterial wall inflammation quantified by (18)F-FDG PET imaging: implications for vascular interventional studies. JACC Cardiovasc Imaging 2016;9:1198–207.
[33] Ripa RS, Hag AM, Knudsen A, et al. (18)F-FDG PET imaging in detection of radiation-induced vascular disease in lymphoma survivors. Am J Nucl Med Mol Imaging 2015;5:408–15.
[34] Hess CB, Rash DL, Daly ME, et al. Competing causes of death and medical comorbidities among patients with human papillomavirus-positive vs human papillomavirus-negative oropharyngeal carcinoma and impact on adherence to radiotherapy. JAMA Otolaryngol Head Neck Surg 2014;140:312–6.
[35] Okoye CCBJ, Tatsuoka C, Parikh SA, Oliveira GH, Gibson MK, Machtay M, et al. Cardiovascular risk and prevention in patients with head and neck cancer treated with radiotherapy. Head Neck 2016.
[36] Addison D, Seidelmann SB, Janjua SA, et al. Human papillomavirus status and the risk of cerebrovascular events following radiation therapy for head and neck Cancer. J Am Heart Assoc 2017;6.
[37] Andersen AS, Koldjaer Solling AS, Ovesen T, et al. The interplay between HPV and host immunity in head and neck squamous cell carcinoma. Int J Cancer 2014;134:2755–63.
[38] Addison D, Lawler PR, Emami H, et al. Incidental statin use and the risk of stroke or transient ischemic attack after radiotherapy for head and neck cancer. J Stroke 2018;20:71–9.
[39] Tahara N, Kai H, Ishibashi M, et al. Simvastatin attenuates plaque inflammation: evaluation by fluorodeoxyglucose positron emission tomography. J Am Coll Cardiol 2006;48:1825–31.
[40] Crouse 3rd JR, Raichlen JS, Riley WA, et al. Effect of rosuvastatin on progression of carotid intima-media thickness in low-risk individuals with subclinical atherosclerosis: the METEOR Trial. JAMA 2007;297:1344–53.